Amino Acid Residues That Influence FcεRI-Mediated Effector Functions of Human Immunoglobulin E†

Ian Sayers,‡,§ Stuart A. Cain,‡ Jillian R. M. Swan,‖ Mark A. Pickett,⊥ Peter J. Watt,⊥ Stephen T. Holgate,○ Eduardo A. Padlan,▽ Peter Schuck,△ and Birgit A. Helm*,‡

Krebs Institute for Biomolecular Research, MBB, University of Sheffield, Sheffield S10 2UH, UK., Health and Safety Laboratory, Broad Lane, Sheffield, U.K., Department of Molecular Microbiology and Department of University Medicine, University of Southampton, Southampton General Hospital, Tremona Road, Southampton, U.K., and Laboratory of Molecular Biology, NIDDK, and Bioengineering and Physical Science Program, OD, National Institutes of Health, Bethesda, Maryland 20892

Received June 18, 1998; Revised Manuscript Received September 4, 1998

ABSTRACT: Immunoglobulin E (IgE) mediates its effector functions via the Fc region of the molecule. IgE binding to and subsequent aggregation of the high-affinity receptor (FcεRI) by allergen plays a pivotal role in type I hypersensitivity responses. Earlier studies implicated the Cε2 and 3 interface and the A−B loop in Cε3 in the IgE−FcεRI interaction. These regions and glycosylation sites in Cε3 were now targeted by site-specific mutagenesis. IgE binding to FcεRI was compared with surface plasmon resonance (SPR) measurements, which assessed the binding of the soluble extracellular domain of FcεRI to IgE. Kinetic analysis based on a pseudo-first-order model agrees with previous determinations. A more refined SPR-based kinetic analysis suggests a biphasic interaction. A model-free empirical analysis, comparing the binding strength and kinetics of native and mutant forms of IgE, identified changes in the kinetics of IgE−FcεRI interaction. Conservative substitutions introduced into the A−B loop have a small effect on binding, suggesting that the overall conformation of the loop is important for the complementary interaction, but multiple sites across the Cε3 domain may influence IgE−FcεRI interactions. Asn394 is essential for the generation of a functional IgE molecule in mammalian cells. A role of Pro333 in the maintenance of a constrained conformation at the interface between Cε2−3 emerged by studying the functional consequences of replacing this residue by Ala and Gly. These substitutions cause a dramatic decrease in the ability of the ligand to mediate stimulus secretion coupling, although only small changes in the association and dissociation rates are observed. Understanding the molecular basis of this phenomenon may provide important information for the design of inhibitors of mast cell degranulation.

Antibodies of the immunoglobulin (Ig)[1] E isotype play an important role in host defense against parasitic infestation (*1*, *2*). In addition to this beneficial role, the synthesis of IgE antibodies has been linked to the development of allergy and asthma. In industrialized countries the prevalence of this disorder is increasing at an alarming rate, and in the absence of effective therapeutic interventions, allergic diseases have a profound socioeconomic impact (*3*).

Strategies that block the initial sensitization of target cells expressing IgE receptors have been explored, following the demonstration that human (h) IgE−Fc-derived fragments can competitively inhibit the binding of the ligand to cells expressing the class specific high- (FcεRI) and low- (FcεRII) affinity receptors (*4*−*20*). Investigations focused on the identification of those regions of the molecules that contribute to the complementary interaction since this information can be expected to contribute to the development of rational anti-allergic drugs (reviewed in ref *15*). The principal determinants for the interaction of IgE with both receptors are located in the Cε3 domain (*14*, *15*). We developed a model structure that predicts the existence of an exposed interdomain region between Cε2/3, which may have limited flexibility and suggested that IgE bends out of plane in this region of the molecule (*21*). Data based on the inhibition of passive cutaneous anaphylaxis tests (PCA) by hIgE−Fc-derived

† This work was supported by grants from the Medical Research Council (U.K.), the European Union, NATO, and the Wellcome Trust. I.S. was a recipient of a BBSRC Studentship. S.A.C. was supported by a Robert Boucher Studentship.

* Author to whom correspondence should be addressed. E-mail: B.Helm@Sheffield.ac.uk.

‡ University of Sheffield.

§ Present address: Asthma Genetics, Wessex Human Genetics Institute, Duthie Building, University of Southampton, Southampton General Hospital, Tremona Rd., Southampton SO16 6YD, U.K.

‖ Health and Safety Laboratory.

⊥ Department of Molecular Microbiology, University of Southampton.

○ Department of University Medicine, University of Southampton.

▽ NIDDK, National Institutes of Health.

△ OD, National Institutes of Health.

[1] Abbreviations: BMGY, buffered glycerol complex medium; BMMY, buffered methanol complex medium; cDNA, complimentary DNA; ECL, enhanced chemiluminescence; FCS, fetal calf serum; FRET, fluorescence resonance energy transfer; h, human; IgE, immunoglobulin E; HBS, Hepes-buffered saline, pH 7.4; PBS, phosphate-buffered saline, pH 7.4; PCR, polymerase chain reaction; RU, resonance units; SDS−PAGE, sodium dodecyl sulfate-polyacrylamide gel electrophoresis; sFcεRIα, soluble extracellular region of the α-chain of the high affinity receptor for IgE; FcεRII, the low affinity receptor for IgE; SPR, surface plasmon resonance.

10.1021/bi981456k CCC: $15.00
Published on Web 10/26/1998

peptides had suggested that this region was essential for the binding of IgE to FcεRI (*12*). We therefore proposed, by analogy with IgG−FcγRI interaction (*22*), that the FcεRI binding region in hIgE might be found in the structural equivalent of the flexible hinge region of other antibodies (*21*). We identified P333, which might facilitate the bending of hIgE, and R334, the homologue to L235 and major effector determinant residue in IgG (*22*), as targets for site-specific mutagenesis (*21*). Others later proposed that the N-terminal 11 amino acid (aa) residues (329−340) in Cε3 are essential for FcεRI binding (*23*, *24*) and that R334 contributes some 23% to the binding energy of IgE−FcεRI (*25*). However, Presta and collaborators (*26*) proposed that six aa residues located in the C−D, E−F, and F−G loops, which have been computed to lie on the outer ridge of the convex face of the Cε3 domain, are involved in FcεRI binding, although their data provide little support for this claim (reviewed in ref 15).

When the fallibility of the PCA test became apparent (*13*, *27*), we re-assessed the biological activity of recombinant IgE-derived peptides (rFcε) in a newly developed assay system where binding and stimulus secretion coupling of hIgE can be assessed (*28*). In this study, we demonstrated that the essential structural determinant for hIgE−FcεRI recognition depends on a consecutive sequence of 11 aa (residues 343−353) in Cε3, computed to form a loop structure (A−B loop) at the interface with the Cε4 domain (*14*). Interestingly, the work of others demonstrated that replacement of the A−B loop in IgE by the homologous sequence from IgG results in loss of receptor recognition (*26*). Furthermore, early studies had shown that pepsin digestion of IgE, which destroys receptor interaction, cleaves the molecule at F349 in the A−B loop (*29*). We demonstrated that N-terminal hIgE sequences could be deleted beyond residue 340 without any significant effect on the association of the ligand with the receptor, although the dissociation rate increased ∼30-fold (*14*). In contrast, C-terminal truncation to P354 accelerates dissociation >3000-fold (*14*). This showed that residues N-terminal to the core sequence and in the inter-Cε2−3 hinge link contribute marginally to the high affinity of the interaction, while residues in the C-terminal part of the Cε3 domain maintain high affinity of interaction by inhibiting the dissociation of the ligand from the receptor. Cε4-specific residues are not required since replacement of this domain by the homologous Cγ3 domain has no effect on the interaction of IgE with FcεRIα (*14*).

We utilized a eukaryotic expression system (*31*, *32*) to express IgE variants since isolation from *Escherichia coli* necessitates in vitro refolding of the ε-chain peptides, which are expressed as insoluble inclusion bodies. Mutations may affect refolding conditions, and it could prove difficult to differentiate between loss of activity as a consequence of such effects and alterations in receptor interaction. Eukaryotic expression also enables an assessment of the role of two prominent glycosylation sites in Cε3. Human IgE is heavily glycosylated and the carbohydrate side chains are N-linked; O-linked glycosylation has not been detected in human E myeloma protein (*29*). Glycosylation may have a function in folding, processing, and secretion of a functional IgE molecule but not in receptor interaction since enzymatically deglycosylated hIgE and hIgE−Fc fragments expressed in *E. coli* still engage both receptors (*7*, *8*, *12*−*14*, *16*). The N394 glycosylation site is of particular interest due to the fact that it is homologous to N297 of IgG_1, which is conserved among immunoglobulin classes. In a model of IgE this residue is buried, in contrast to N265 and N371, which are surface exposed (*32*).

A major objective of the present study was to answer the question whether residues in the interdomain region between Cε2−3 and in the A−B loop of Cε3 contribute directly to receptor binding through, for example, electrostatic interaction, or whether they are required to maintain a conformation that is essential for the correct docking of the ligand into the receptor. In the structural model for hIgE, the A−B loop is one residue shorter than the corresponding loop in IgG, using the X-ray structure on which the model is based (*33*). In the region of the one residue deletion between D347 and L348, the model predicts an unusual and distinctive 'kink' involving F346, D347, and L348, which is retained following simulated annealing (2000−300 °C) (E. A. Padlan, unpublished observations). We hypothesized that if this kink is not an artifact of modeling, then it might be important for the binding to the receptor, and consequently, these residues were targeted by mutagenesis.

The aa substitutions generated in this study were designed to incorporate the homologous rodent residues or to replace an aa by the most conserved residue of the same charge and/or opposite charge, e.g., R by K and D by E and K in order to minimize potential distortions in the overall conformation. To assess the role of P substitution, A was chosen because it is similar in size and hydrophobicity. This should result in a molecule that has similar contacts with the receptor, if this were the residue's only contribution. If P333 contributed to the interaction by its restriction on structure, a P to G mutation should further substantiate this since it constitutes an exchange of the conformationally most restricted by the most unrestricted aa.

In the present investigation, we studied the functional consequences of site-specific mutagenesis by assessing the binding of native hIgE and rFcε to rat basophilic leukemia cells transfected with hFcεRIα (RBL-J41) and compared data obtained from cell binding studies with surface plasmon resonance (SPR) measurements. Kinetic values were initially calculated assuming a simple 1:1 pseudo-first-order interaction proposed for the binding of rat IgE to FcεRI (*34*). A more detailed analysis of the binding and dissociation events by SPR was carried out. This showed that the application of monophasic kinetics to the interaction is inadequate. We also assessed the ability of the mutant IgE molecules to mediate stimulus secretion coupling.

Our observations suggest that the overall conformation of the A−B loop in Cε3 is important for the correct docking of the ligand into the receptor. They also point to the role of P333 as an important determinant for the maintenance of a relatively rigid inter-Cε2−3 hinge link region (*21*) and show that a decrease in structural constraints in this region of the IgE molecule has a profound influence on the ability of the ligand to mediate receptor aggregation and secretory responses.

MATERIALS AND METHODS

Gene Constructs and Site-Directed Mutagenesis. The numbering scheme for the hε-chain and FcεRIα amino acid

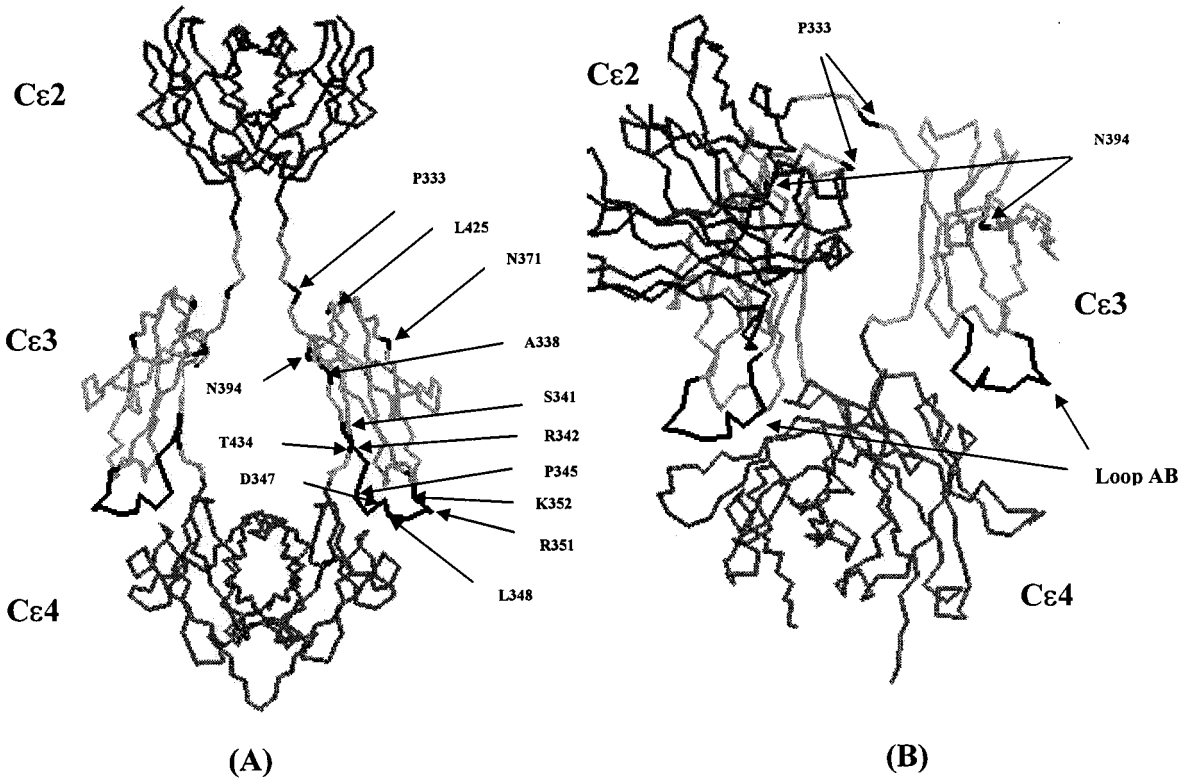

FIGURE 1: Protein engineering of the human IgE Fc region. Specific Cϵ3 residues targeted and positions within a coplanar (A) and bent (B) model of the human IgE Fc region (*15*) are shown in black and are labeled. The illustration highlights regions of interest, the Cϵ2−3 interface, Cϵ3 glycosylation sites, and A−B loop, including residues Pro343−Ser353 previously identified as the essential sequence required for IgE/FcϵRIα interaction (*14*).

has been maintained (*12*−*16*). The sequences of rodent and hIgE are based on our own data, which agree with those published by Kabat et al. (*35*) but are at variance with those shown in Figure 1 of Henry et al. (*25*). The procedure for the construction of mutant recombinant IgE molecules has been described previously (*14*); mutagenic primers were designed to incorporate the minimum base pair substitutions for the generation of the desired aa substitution(s), primers ranged between 15 and 55 bp in length.

For the construction of the soluble form of FcϵRIα chain extracellular (EC) domains, a modified *Pichia pastoris* pPIC9 expression vector (Invitrogen) was used. This contained the Tn903 kan^r gene inserted into the *Nae*I site of pPIC9, which conferred resistance to G418 (designated pPIC9K). The gene fragment coding for the extracellular region of FcϵRIα (residues 1−172) was generated by PCR as described above using the FcϵRIα cDNA cloned into pGEM3Zf as a template (5′ Ria-1 GGCCGGGAATTCATGGTCCCTCAGAAACCTAAG, 3′ Ria-172 GGATCCGCGGCCGCTCAAGCTTTTATTACAGTAATGTT). The resultant 542 bp fragment was blunt cloned into the *Sma*I site of pUC18 for gene sequencing and then subcloned into the pPIC9K expression vector using *Eco*RI and *Not*I to generate pPIC9k−αEC. The gene was sequenced again prior to transformation into the *P. pastoris* strain GS115 to ensure that the DNA was in frame for expression. Bacterial strains JM109 and TG1 were used for the propagation of plasmid DNA.

Gene Expression/Cell Culture. Plasmids containing mutant V_{NP}Hϵ constructs (approximately 25 μg) were linearized using *Pvu*I and transfected into the J558L plasmocytoma cell line by electroporation. J558L cells were cultured in Dulbecco's modified eagles medium (DMEM) [10% fetal calf serum, penicillin (100 U/mL)/streptomycin (100 μg/mL), and gentamicin (50 μg/mL)]. Exponentially growing cells were isolated by centrifugation, washed twice with DMEM in the absence of any supplements, and resuspended to give 10^7 cells/0.8 mL. The linearized DNA was mixed with the 0.8 mL of cell suspension, transferred into a 0.4 cm gap electroporation cuvette (Bio-Rad), and placed on ice for 10 min. A single 250 V, 960 μF pulse was applied (Bio-Rad Genepulser), and the cells were returned to the ice for 10 min. Twenty milliliters of fresh medium was added, and the cells were plated into 24 well plates (0.5 mL/well). After 48 h, spent medium was carefully aspirated, and selection medium was added [containing mycophenolic acid (1 μg/mL), xanthine (250 μg/mL), and hypoxanthine (15 μg/mL)]. This procedure was repeated every 3−4 days, and clones were visible after 15 days. Cloning, using limiting dilution and screening by a sandwich enzyme-linked immunosorbant assay (ELISA), isolated high secreting clones. A mouse anti-human IgE capture antibody LE27, (anti-Cϵ4, gift of Prof. B. Stadler, University of Bern, Switzerland) and a commercial HRP-anti IgE detection antiserum (Dako) were used for this procedure. Protein expression was also analyzed by SDS−PAGE and Western blotting using the same commercial HRP-conjugated anti-human ϵ-chain antibody (Dako). High secretion variants were grown in stirred, aerated vessels (1−4 L of culture) until the cells were confluent. The supernatant was collected, filtered, and concentrated 10× using a Millipore Minitan System with a 30 kDa MW cutoff.

For the production of soluble, secreted sFcϵRIα the pPIC9K−αEC vector (10−20 μg) was linearized using *Sac*I and transformed by electroporation into the *Pichia pastoris* strain GS115 (Invitrogen). The transformation conditions

used were as recommended by Invitrogen and involved a single pulse of 1500 V, 25 μF, 200 Ω applied to 90 μL of DNA/cell suspension in a 0.2 cm gap electroporation cuvette (Bio-Rad) (*36*). The transformed cells were first selected by plating onto MD plates in order to detect HIS^+ transformants, and then high copy number clones were isolated by plating the HIS+ transformants onto YPD plates containing increasing concentrations of G418 (0.5, 1.0, 1.5, and 2.0 mg/mL). G418-resistant colonies were isolated, and sFcϵRIα expression was assessed by small-scale expression with methanol induction using BMGY and BMMY media in 250 mL baffled flasks. Supernatants were analyzed by SDS−PAGE and ECL detection using a monoclonal anti-hFcϵRIα chain antibody 15.1 (gift of J. P. Kinet, Harvard, Boston, MA). For the large-scale production of sFcϵRIα, the fermentation was scaled up into 2.5 L baffled flasks containing 500 mL of media. After 2−3 days of methanol induction, the supernatant was isolated by centrifugation, filtered, and concentrated 10−20× using a stirred ultrafiltration cell with a 10 kDa MW cutoff (Amicon). In an analogous way, a control cell line was generated by transformation with the pPIC9K vector in the absence of the FcϵRIα gene.

Detection of Recombinant IgE by ELISA. A sandwich ELISA was used for the detection and semiquantification of recombinant IgE present in cell supernatants. On the day prior to analysis, a 96 well assay plate (Falcon) was coated with a mouse monoclonal anti-hIgE Cϵ4 antibody (LE27) at a concentration of 10 μg/mL in 0.1 M carbonate/bicarbonate buffer pH 9.6 (100 μL/well). The plate was incubated overnight at room temperature and then washed three times with wash buffer (0.05% Tween/PBS) followed by 200 μL of a blocking solution (5% milk powder/0.05% Tween/PBS). After a 2 h incubation at 37 °C, the plate was washed, and a number of dilutions of the samples were added, 100 μL/well. A standard graph was generated using commercially available recombinant IgE (Serotec, 0.001−50 μg/mL). Following a second 2 h incubation at 37 °C, the plate was washed, and 100 μL of anti-hIgE HRP conjugated antiserum (DAKO, 1/500 dilution in blocking buffer) was added to each well. Following a further 2 h incubation at 37 °C, the plate was washed, and HRP activity was detected by adding 100 μL/mL of OPD buffer [0.4 mg of *O*-phenylenediamine (OPD), 12 μL of H_2O_2 in 0.2 M citrate/phosphate buffer, pH 5.0]. After 5−10 min, the color reaction was stopped by adding 50 μL/well 2 M H_2SO_4. The absorbance (OD) at 492 nm was determined using an ELISA plate reader (Milenia Kinetic Analyzer), and test samples were calculated from the constructed absorbance vs concentration graph. Appropriate controls were included at each stage of the assay in order to correct for background.

Recombinant/Chimeric IgE and sFcϵRIα Purification. Each recombinant IgE protein was purified from tissue culture supernatant employing established procedures (*31*). Purified antibodies were dialyzed extensively against PBS to remove hapten from the variable region, filtered through a 0.45 μm filter (Amicon), and concentrated using ultrafiltration (Amicon Centriplus 50).

sFcϵRIα was affinity adsorbed onto rat IgE coupled to Sepharose (Sepharose, Pharmacia). The sFcϵRIα was bound to the resin slurry by incubation overnight on a rotating platform at 4 °C and eluted with 0.2 M glycine buffer, pH 2.8, followed by immediate neutralization using 1 M Tris-HCl, pH 8.0.

The IgE variants and sFcϵRIα were quantified on the BIAcore 2000 system using BIAconcentration software. Known concentrations of IgE (Serotec) and an affinity purified preparation of FcϵRIα were employed to construct a dose/response curve on the biosensor. The samples were analyzed for a number of dilutions, and the concentrations were calculated. A description of the BIAcore system is given below.

IgE-Mediated Stimulus Secretion Coupling in Rat Basophilic Leukemia Cells Transfected with the α-Chain of the Human High Affinity Receptor. Recombinant IgE molecules were assessed for their ability to bind to and aggregate the hFcϵRIα chain constitutively expressed on the surface of the RBL-J41 cell line, which also expresses the subunits of rat FcϵRI (*36*). RBL-J41 and the parental RBL-2H3.1 (*37*) cell lines were used to evaluate the ability of recombinant IgE variants to support the release of cellular mediators, monitored by the secretion of [^{3}H]5-hydroxytryptamine [5-HT] as described previously (*28*). Since peak secretion via human and rat receptors varied by up to 10% between experiments, the data set was normalized to the peak secretion effected via triggering through the endogenous rodent receptor, which was included as an internal control in each experiment.

Each hIgE variant (1 μg/mL) was assessed for its ability to mediate stimulus secretion coupling via the hFcϵRIα chain using a hapten cross-linking agent (NIP−HSA 0.1−10000 ng/mL) or a commercial anti-ϵ-chain antiserum (DAKO, dilution 1/100−1/5000).

Ligand-Binding Studies using Surface Plasmon Resonance (SPR). A biosensor-based analytical system (BIAcore Inc, Uppsala, Sweden) was used to analyze the kinetics of interaction between IgE variants and sFcϵRIα. Binding events to surface immobilized sites are detected in real-time by a change in local refractive index, which is measured in arbitrary units (termed resonance units, RU). A mouse monoclonal anti-hIgE antibody LE27 [∼13 000 resonance units (RU) (13 ng/mm^2)] was immobilized to the CM5 sensor surface via amino groups and used to capture hIgE. Binding studies were carried out at 25 °C. For each IgE variant analyzed, seven experimental cycles were performed, including the control cycle. Each cycle consisted of binding a constant amount of the IgE variant followed by a series of fixed concentrations of sFcϵRIα. The IgE variants were diluted in HBS [10 mM HEPES, pH 7.4, 3.4 mM EDTA, 150 mM NaCl, 0.005% (v/v) surfactant P20] to a final concentration of 10 μg/mL and bound to the capture antibody to provide between 600 and 3300 (0.6−3.3 ng/mm^2) of surface-bound ligand. sFcϵRIα, at concentrations of 100−600 nM were passed over the captured IgE variant at a flow rate of 15 μL/ml for 3 min. Dissociation was monitored for a further 3 h. A total of 10 μL of 10 mM glycine−HCl, pH 2.2, was used to remove IgE−sFcϵRIα complexes and to prepare the surface for the next analytical cycle. The sFcϵRIα was added as secreted supernatant from tissue culture, and medium from the control cell line was included in a control experiment. All sensorgrams were corrected for dissociation of IgE from the LE27 antibody by subtraction of the control curve.

Binding Analysis Based on an Assumed 1:1 Pseudo-First-Order Interaction. The apparent rate constants k_a and k_d for

the IgE−sFcεRIα interaction were calculated using BIAevaluation software (BIAcore, Uppsala, Sweden) in two alternative analysis strategies. First, for the determination of effective apparent rate and equilibrium constants for the overall binding process, BIAevaluation v2.1 was used (*38*). The apparent dissociation rate constant was determined by selection of the linear parts of a logarithmic plot $\ln(R(t_0)/R)$ vs t of the dissociation sensorgrams [where $R(t)$ denotes the sensor signal]. Based on the relationship $\ln (R(t_0)/R) = k_d(t - t_0)$, the slope of the data subset gives an apparent dissociation rate constant. Similarly, an apparent association rate constant was determined by taking the slope of a time derivative plot dR/dt vs t of the association phase, which obeys $k_a c + k_d$ in a pseudo-first-order reaction (*38*). For a more detailed global kinetic analysis with the 1:1 pseudo-first order model, BIAevaluation v3.0 was used. The complete set of dissociation phases over the entire 8000 s of observation time was fitted globally with the pseudo-first-order rate equation under the constraint to give a single apparent dissociation rate constant. The set of association phase data were fitted over the entire observation time using the pseudo-first-order rate equation, calculating the apparent association rate constant.

Empirical Comparative Analysis of the Binding of Different IgE Variants. The observed binding kinetics are biphasic (i.e., the dissociation curves show initially a phase with a signal decrease steeper than the best-fit single exponential, followed by a phase of slower dissociation). Since this does not appear to be due to mass transport limitations or artifacts of immobilization (see below), this indicates a more complex interaction scheme. In addition, dissociation and rebinding processes of IgE from the capturing antibody within the gel matrix and along the sensor surface causes small signal drifts, complicating the observed kinetic process. In particular, the correction for leakage of the captured IgE and IgE−sFcεrIα is not precise and reproducible enough to allow a reliable kinetic analysis on a level detailed enough to discriminate between possible binding mechanisms underlying the biphasic kinetics. Therefore, an empirical and robust semiquantitative analysis was performed, which describes general trends of the association and dissociation kinetics, under conditions used in the experiments. Since the following analysis obviously does not describe the detailed process of the binding of IgE to its receptor, the obtained estimates cannot be interpreted as bimolecular rate constants. However, they allow a comparison of the effects of mutations on the overall characteristics of the binding process. Three empirical measures for affinity and binding kinetics were applied.

First, the fractional occupation of IgE binding sites after an injection of 600 nM sFcεRIα for 180 s was measured. To eliminate contributions from nonspecific binding and sample refractive index, the signal increase due to bound sFcεRIα was measured immediately after injection of sFcεRIα. This value was divided by the signal increase during capture of IgE. This ratio is a measure of the fractional occupation of binding sites. Since the signal of the 600 nM injection after 180 s is close to steady-state plateau binding, the fractional binding can be regarded as a gross empirical measure of the affinity of IgE−sFcεRIα interaction and can be compared for the different mutations. Second, the association kinetics during the first 100 s during the injection of sFcεRIα was fitted to a single exponential in order to obtain an empirical binding rate (k_{obs}) dependent on the sFcεRIα concentration. These curves ($k_{obs}(c)$) can serve as a model-free empirical measure for kinetic properties of the interaction in the association phase. Third, the first 300 s of the dissociation kinetics were analyzed using a single-exponential model $R(t) = R(t_0) \exp[k_d^*(t - t_0)]$. The empirical dissociation rate constant k_d^* may not be identical to a true molecular dissociation rate constant but gives an empirical comparative measure of the dissociation properties of the mutants. In principle, this empirical approach could be extended to a purely descriptive double-exponential analysis. However, the reproducibility of IgE leakage, the errors involved in double-exponential modeling due to cross-correlation of the parameters, and the selection of the data subset included in the analysis prohibit the empirical comparison of small effects of the mutations on a level of detail higher than in the single-exponential approach described here.

RESULTS

Design of Mutant Forms of IgE. The goal of this study was to gain information concerning residues in human IgE that influence the interaction with FcεRI in the context of a model we proposed for a planar and bent conformation of IgE (*15*). Table 1 provides an overview of the rationale for each of the substitutions. Additional mutations to those engineered were also introduced in some constructs, due to lack of proof-reading ability of the polymerase, and their effects were evaluated.

Expression of Variant Forms of IgE. Plasmids encoding native and mutant form of IgE−V_{NP}−Hε were stably expressed in J558L plasmocytoma cells using established procedures (*14*). High secreting clones were selected by cloning at limiting dilutions and screening by ELISA. Expression levels varied between 0.1 and 30 μg/mL. Purified antibodies displayed identical characteristics in SDS−PAGE/ECL analysis shown in previous studies (ref *30*, data not shown).

Expression of sFcεRIα in Yeast Pichia pastoris. The data for sFcεRIα production in the methylotropic yeast *P. pastoris* will be presented elsewhere (Cain et al., manuscript in preparation). Following affinity purification, a diffuse band of 45−55 KDa, corresponding to the heterogeneously glycosylated form of FcεRIα, was observed. This band reacted with a mouse anti-hFcεRIα monoclonal antibody (*15*−*1*) and protein sequence analysis confirmed that this was the soluble extracellular domain of human FcεRIα (data not shown).

Kinetic Analysis of the IgE Variant−sFcεRIα Interaction. Figure 2 shows a typical sensorgram used for the determination of kinetic constants for the wild-type recombinant IgE−sFcεRIα interaction. This procedure was employed for all other IgE variants. The sensorgrams obtained were highly reproducible and clearly demonstrate capturing of the IgE to the immobilized antibody as well as its interaction with sFcεRIα. Kinetic analysis applying a pseudo-first-order model as outlined by Karlsson (*38*) leads to apparent rate constants for each concentration used, as shown in Table 2. The k_a and k_d values obtained for native IgE shown in Table 2 compare well with previously published determinations (*14*,

Table 1: Rationale for Site-Directed Mutagenesis of Residues in the hIgE Cϵ3 Domain[a]

hIgE variant	rationale for mutation
	Cϵ2-3 Interface
Pro333−Ala (*F321L)	Pro333 is conserved in human, rat, and mouse IgE; mutation to Ala may remove a fixed bend while maintaining the hydrophobicity and size of the residue
Pro333−Gly	mutation may remove additional conformational constraints and introduce the flexibility associated with a Gly residue
	A−B Loop
R16	homologous rat residues (aa341−356) grafted into the human Fc region to replace A−B loop; can the mutation confer binding to the rodent high affinity receptor, which does not engage human IgE?
Ser341/Arg342−Ileu/Pro (*A338V, L425P, T434A)	replacement of human residues by the homologous rat amino acids in IgE−Fc; will the mutation confer binding to rodent FcϵRI?
Pro345−Ala	Pro345 is conserved in human, mouse, and rat IgE; mutation to Ala removes a potentially fixed bend while maintaining the hydrophobicity and size of the residue
Asp347−Asn	Asp347 is conserved in human, mouse, and rat IgE; mutation to Asn maintains the size of the amino acid side chain but alters the charge
Asp347−Glu	mutation to Glu maintains the charge of the residue but increases the length of the side chain
Leu348−Ileu	Leu348 is conserved in human, mouse, and rat IgE; mutation to Ileu is highly conservative, changing only the position of a methyl group on the side chain
Arg351−Lys	Arg351 is not conserved in mouse and rat IgE; rodent homologue is Asn; mutation to Lys maintains the hydrophilic nature of the residue while decreasing the length of the side chain
Lys352−Gly (*E270G)	Lys352 is not conserved; the rodent homologue is Gly
	Glycosylation Sites
Asn371−Thr	Asn371 is conserved in human and mouse IgE; the rat homologue is Thr; mutation to Thr may change the glycosylation from type N to O or inhibit glycosylation
Asn394−Thr	Asn394 is conserved in human, rat, mouse IgE, and in other Ig classes; mutation to Thr may alter glycosylation from type N to O or inhibit glycosylation
Asn371/394−Thr (*G368R)	double glycosylation site mutation
wild type	produced as an internal control for the system

[a] Engineered mutations are listed (in regions targeted) including additional mutations* introduced during generation (see text).

19, *39*, *41*, *42*) where the binding of hIgE to cell surface FcϵRI was measured. These data are however based on the assumption that IgE−FcϵRI interaction is a simple 1:1 pseudo-first-order interaction.

The results of a more refined kinetic analysis applying global fitting techniques are shown in Figure 2, panels C and D. The relatively large deviations from the best fit of a pseudo-first-order model to the data clearly show that the kinetic binding data of IgE−FcϵRI interaction provided by the SPR biosensor does not fit a simple 1:1 binding model. This is also reflected in the nonlinear dependence of k_{obs} on concentration, as shown in Figure 3. For a pseudo-first-order reaction, the relationship of $k_{obs}(c)$ is linear, and the slope gives the chemical on-rate constant, while an extrapolated rate $k_{obs}(0)$ is equal to the dissociation rate constant (*43*). For the IgE−FcϵRI interaction, this is clearly not fulfilled (Figure 3), as is evident from the biphasic characteristics of the sensorgrams.

The observed biphasic kinetics can be empirically modeled by double exponentials (data not shown). Such kinetics can only be meaningfully interpreted on the basis of a detailed model for the interaction, which is currently unavailable. In addition, baseline subtraction to account for leakage of IgE from the surface was found to be not precise enough for a detailed kinetics analysis employing a complex model. For this reason, a simple and robust model-free descriptive analysis was used for the analysis of the different IgE variants. While the obtained values are not identical to bimolecular rate constants, the observed relationship $k_{obs}(c)$ still contains crucial information on the association properties and shows clear effects of the mutations (Figure 3). Similarly, the empirical dissociation rate constant k_d* and the fractional binding after completion of the 600 nM injection, demonstrate the distinct effects of mutations on equilibrium properties and dissociation process of the formed IgE−FcϵRI complex (Figure 4). The dissociation rate constant k_d* during the first 300 s is a lower limit for the true bimolecular dissociation rate constant. It may, however, be a quantity compounded by, for example, the kinetics of possible conformational changes.

On the basis of this analysis, all samples of native IgE show curves $k_{obs}(c)$ relatively consistent to each other and to most of the mutants (Figure 3). The largest effect was found for S341I/R342P*, which showed significantly slower association kinetics and an order of magnitude increased dissociation kinetics, consistent with an order of magnitude reduced fractional saturation. IgE variants with P333A and P333G mutations also showed significantly increased dissociation, a slightly slower initial association process, but little effect on fractional saturation. IgER16 showed the fastest association process and highest fractional saturation, while its dissociation rate is nearly identical to that of the wild type. N371T exhibits slightly slower association kinetics, dissociation kinetics, and fractional binding. The N394T variants (N394T, N371/394T*) showed no detectable binding activity.

Establishment of a Rat Basophilic Leukemia (RBL) Cell Line Supporting Constitutive Expression of the α-Chain of Human FcϵRI and Stimulus Secretion Coupling by Native and Mutant Forms of Human IgE. The RBL-J41 constitutively expresses ~10 000 human α-chains per cell and was employed to assess the coupling of IgE-mediated receptor

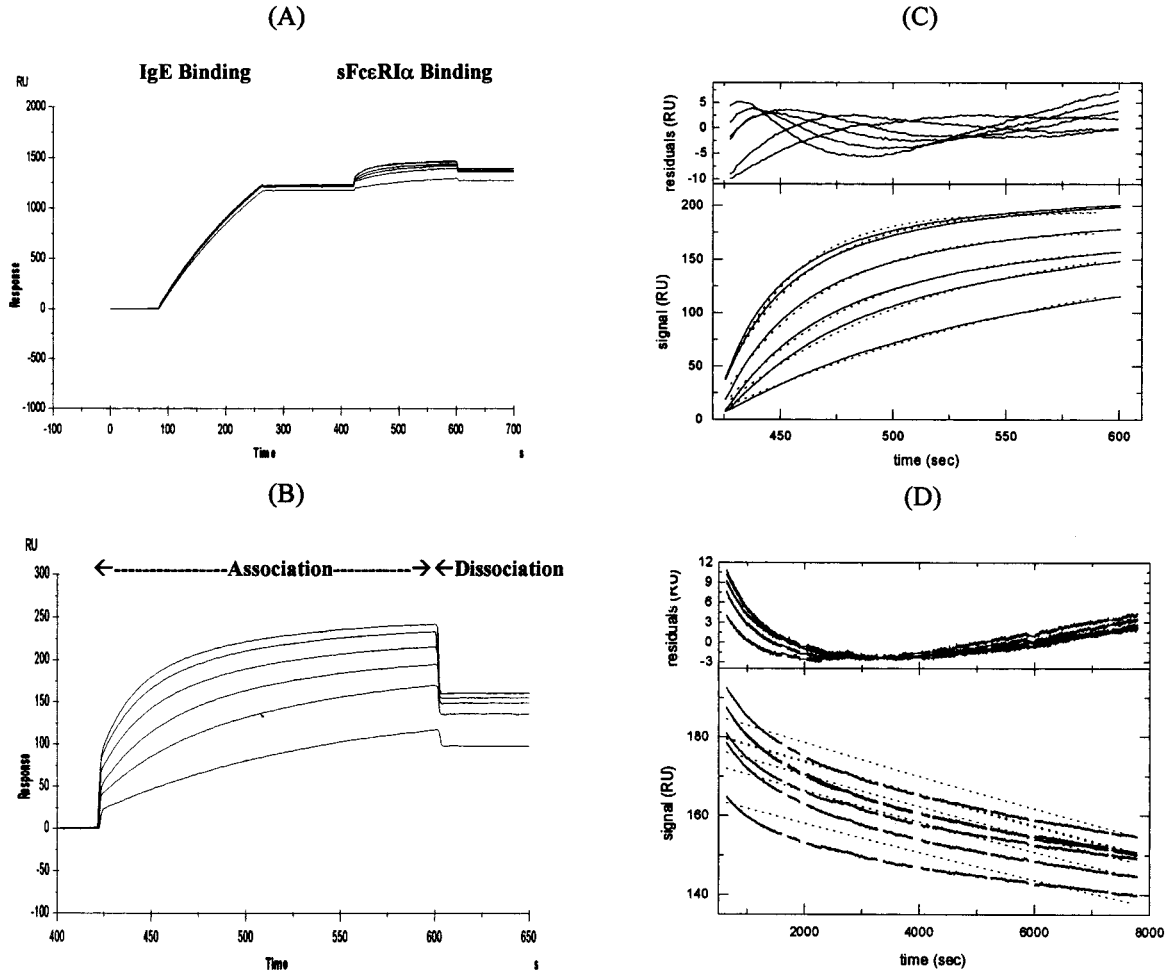

FIGURE 2: SPR analysis of the hIgE−sFcεRIα interaction. The figure illustrates the analysis of the wild-type IgE interaction; all other variants were analyzed in an analogous manner, see Materials and Methods. Panel A: Sensorgrams tracing the repeated injection/binding of IgE (45 μL injection of 10 μg/mL at a flow rate of 15 μL/min) to the immobilized LE27 monoclonal anti Cϵ4 antibody (~1300 RU immobilized) followed by the binding of sFcεRIα for the concentration range 100−600 nM (45 μL kinject). Note that the dissociation following the sFcεRIα binding was monitored for 3 h whereas in the figure the dissociation has been truncated. Panel B: IgE−sFcεRIα interactions for the different sFcεRIα concentrations. For both the LE27−IgE and IgE−sFcεRIα interactions, a binding event can be followed with time, resulting in an increase in resonance units and an elevated RU level maintained at the end of the injection. Panel C: Sensorgrams of the association phase of FcεRIα binding to surface-bound IgE at a concentration of 100−600 nM (bottom, solid lines), best global fit based on a 1:1 pseudo-first-order model (bottom, dotted lines), and residuals of the fit (top, solid lines). Panel D: Sensorgrams of the dissociation phase of FcεRIα−IgE interaction (bottom, solid lines), best global fit based on a 1:1 pseudo-first-order model (bottom, dotted lines), and residuals of the fit (top, solid lines).

activation to degranulation (*36*) and to detect any changes in the effector functions of IgE variants. Data for native IgE and the 13 IgE variants generated in this study are summarized in Figure 5. Panel A illustrates that the ability of the IgER16 variant (*14*) to stimulate mediator secretion following sensitization and challenge with NIP−HSA or anti-ϵ-chain antibody is essentially indistinguishable from native hIgE. Surprisingly, replacement of P333 by A or G has only a modest effect on binding to the cellular receptor (Table 2) but profoundly influences the capability of the mutant ligands to induce mediator secretion following cross-linking by antigen or anti-IgE. The P333A* mutant showed an approximately 50% reduction in its ability to couple a cross-linking stimulus to mediator secretion as compared to native IgE. This indicates that this mutation inhibited the ability of the molecule to aggregate hFcεRIα in response to an antigen or anti-IgE-mediated cross-linking stimulus (Figure 5A). It is unlikely that this effect is influenced by an additional mutation (F321L) since the single P333G point mutation is associated with a complete loss of stimulus secretion coupling.

Data in Figure 5B show secretion levels obtained following the analysis of a series of A−B loop variants: D347N, D347E, P345A, R351K, and L348I. Interestingly, none of the A−B loop variants altered the hFcεRIα binding and aggregation activity as compared to native IgE. Figure 5C shows the dose/response challenge data for RBL-J41 cells sensitized with the K352G*, N371T, N394T, and N371T/N394T*. It demonstrates that IgE-mediated secretion levels for the K352G* and N371T variants are in excellent agreement with the control values obtained for native IgE. IgE mutants that contain the N394T (N394T, N371T/N394T*) substitution demonstrated no detectable binding activity and do not support secretion of cellular mediators.

DISCUSSION

Kinetic Analysis. In the current investigation, measurements for the binding of hIgE to RBL cells transfected with

Table 2: Kinetic Constants for the Human IgE−FcεRIα Interaction[a]

ligand	assay	k_a (M^{-1} s^{-1})	k_d (s^{-1})	K_A (M^{-1})	ref
		Current Determinations			
recombinant IgE	SPR 25 °C, pseudo-first-order	7.4×10^4	2.7×10^{-6}	2.78×10^{10}	
recombinant IgE (Serotec)	SPR 25 °C, pseudo-first-order	7.2×10^4	3.1×10^{-6}	2.28×10^{10}	
recombinant IgE	SPR 25 °C, empirical	$\sim 4-5 \times 10^4$	$\sim 10^{-4}$	$\sim 10^9$	
recombinant IgE P333A	cellular, 25 °C	1×10^4	2×10^{-5}	5×10^9	
recombinant IgE P333A	SPR 25 °C, pseudo-first-order	4.85×10^4	1.02×10^{-5}	4.5×10^9	
recombinant IgE P333G	cellular, 25 °C	8.2×10^4	2.8×10^{-5}	3×10^9	
recombinant IgE P333G	SPR 25 °C, pseudo-first-order	4.36×10^4	1.4×10^{-5}	3.12×10^9	
		Previous Determinations			
human IgE	celluar, 25 °C	8.0×10^4	9.0×10^{-6}	0.90×10^{10}	*39*
myeloma IgE	cellular, 25 °C	1.1×10^5	1.3×10^{-5}	0.85×10^{10}	*40*
recombinant IgE	cellular, 25 °C	1.8×10^4	3.0×10^{-6}	0.62×10^{10}	*19*
IgE−PS	cellular, 25 °C	1.1×10^5	1.1×10^{-5}	1.00×10^{10}	*43*
myeloma IgE	cellular, 25 °C	3.1×10^5	9.0×10^{-6}	3.40×10^{10}	*42*
recombinant IgE	cellular, 22 °C	3.1×10^5	1.3×10^{-5}	2.40×10^{10}	*14*
GST−Fcε 326−547	cellular, 22 °C	4.1×10^5	2.95×10^{-5}	1.37×10^{10}	*14*
GST−Fcε 340−547	cellular, 22 °C	4.2×10^5	9.8×10^{-5}	4.35×10^9	*14*
GST−Fcε 226−354	cellular, 22 °C	4.3×10^5	6.02×10^{-3}	7.14×10^7	*14*
myeloma IgE	SPR 25 °C, biphasic	k_{a1} 3.5×10^5	k_{d1} 1.4×10^{-2}	K_{A1} 2.5×10^7	*25*
		k_{a2} 8.6×10^4	k_{d2} 3.6×10^{-4}	K_{A2} 2.4×10^8	

[a] Kinetic constants, calculated using the pseudo-first-order and empirical SPR analysis, are shown. A summary of previously determined values is included for comparison. Pseudo-first-order analysis of the kinetics of native hIgE binding to the cellular receptor and SPR data produced values that are in excellent agreement and also applicable to IgE mutants P333A/G. More complex binding kinetics became apparent following a detailed analysis of SPR data (see text). Also included are the kinetic constants for several key hIgE−Fc fragments that have been expressed as GST fusion proteins.

the α-chain of the hFcεRI were complemented by a biosensor-based analytical system, which is a relatively new technique applied to the study of ligand−receptor interaction (*4*). Others assessed the binding of IgE−Fc to IgG−Fc−$(Fc\epsilon RI\alpha)_2$ chimeras and reported that the affinity constant determined by SPR is about 10-fold lower than that obtained from cell binding assays. They proposed that this decrease could be due to the requirement of additional subunits of the FcεRI complex in order to confer identical affinity on the interaction (*25*). However, a complicating factor in the direct comparison of cell binding studies and SPR data is that cell binding studies rely on the assumption that IgE−FcεRI interaction follows simple 1:1 first-order kinetics, whereas the more detailed kinetic analysis of SPR data reveals biphasic interaction kinetics. While several different mechanisms could be responsible for biphasic kinetics, Henry et al. (*25*) concluded that two independent classes of binding sites exist. Although our data are also indicative of a biphasic binding mode, we demonstrate that when equal criteria, i.e., pseudo-first-order kinetics are applied to the interaction, identical kinetic constants are obtained from cell binding and SPR studies. Similar observations were made when the kinetics of binding of the P333A/G mutants to the cellular receptor were compared with SPR measurements (Table 2). Our analysis, therefore, does not indicate that additional receptor subunits such as the γ-chain increase the affinity between IgE and FcεRI.

On the basis of our data and on those of others (*25*), common potential artifacts in SPR experiments can be ruled out as a source of biphasic kinetics. Analysis of the data from fractionation and re-injection experiments (Figure 5; Table 6 in ref *25*), in the context of a model for mass transport limited kinetics (*45*), shows that transport limitation and rebinding cannot be the cause of the biphasic dissociation (data not shown). Furthermore, immobilization artifacts seem very unlikely because the biphasic kinetics have been observed with different chemical cross-linking techniques for sFcεRIα (*25*), as well as with the antibody capture of the IgE in the present study. Also, heterogeneity of one of the binding partners can be ruled out as the primary origin of biphasic binding. Finally, although steric hindrance artifacts in the SPR sensor could, in principle, be a source of biphasic binding in the association phase (*46*), it should leave the dissociation phase less affected and would be absent in the experiments with lower surface coverage. Therefore, the molecular mechanism of the interaction must account for the biphasic binding kinetics.

One major point of criticism of the data interpretation by Henry et al. (*25*) is that the empirical fit of each sensorgram phase with double exponentials is taken as evidence for two different independent binding sites with different affinities (see Table 2). On the other hand, the interaction has a 1:1 stoichiometry, and in the presence of two independently acting interactions on the same molecules, one should expect avidity effects through entropic co-localization factors leading to several orders of magnitude higher overall apparent affinity than those for the individual interactions (*47*). This, however, does not conform to the observations. Furthermore, in the double-exponential analysis of Henry et al., it is assumed that the fast rate constants, labeled k_{a1} and k_{d1}, and the slow rate constants, labeled k_{a2} and k_{d2}, respectively, belong to two independent binding sites with equilibrium $K_{a1} = k_{a1}/k_{d1}$ and $K_{a2} = k_{a2}/k_{d2}$ (*25*). This cannot be deduced from the analysis of the independent kinetic curves and their decomposition into double exponentials alone (*48*). Thus, the numerical values of the rate and affinity constants and the interaction mechanism implied in the analysis of Henry et al. (*25*) are doubtful.

A possible alternative mechanism responsible for the biphasic binding kinetics could be a conformational transition between two states of the complex. Observations by Ortega et al. (*49*) and structure−function studies on IgE−FcεRI interaction suggest that a conformational rearrangement in

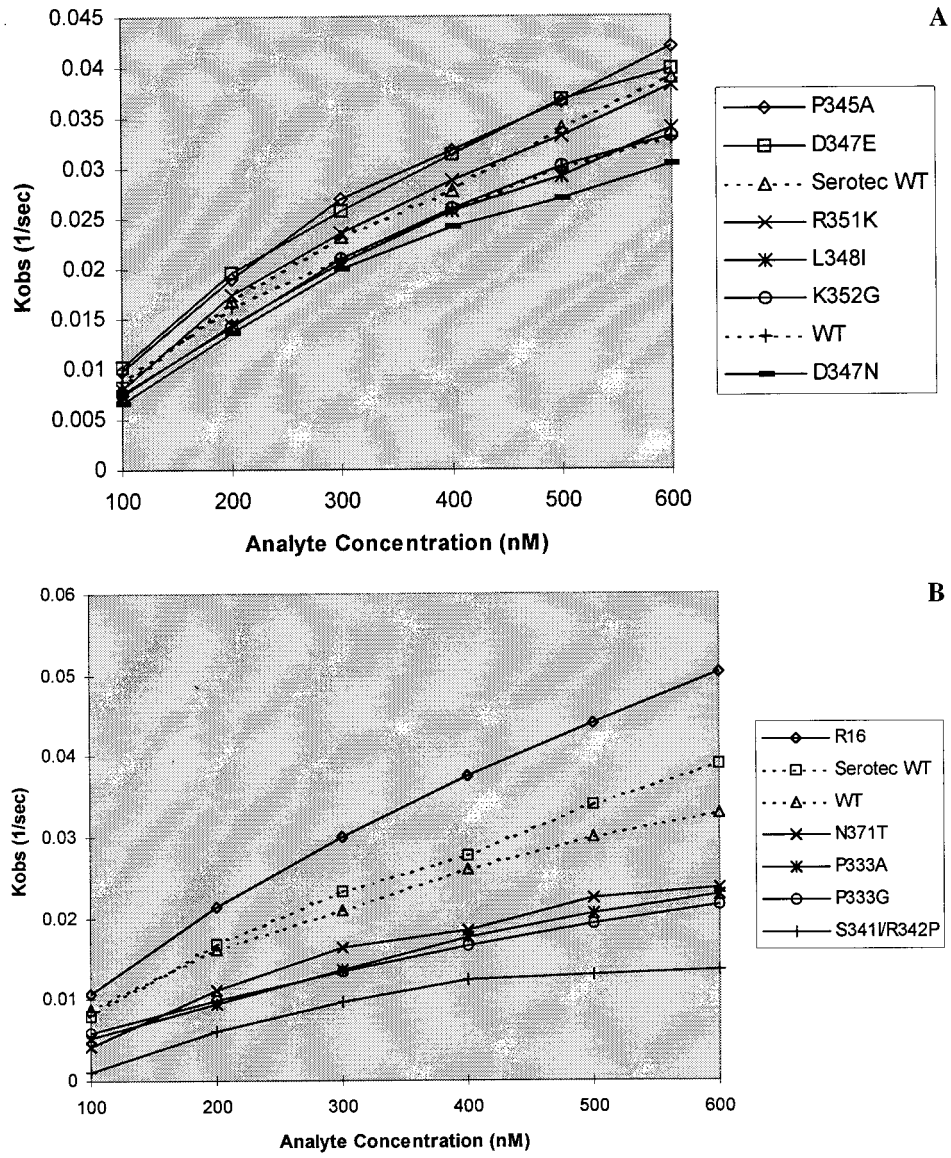

FIGURE 3: K_{obs} vs concentration plots for hIgE variants. The association kinetics during the first 100 s during the injection of sFcεRIα was fitted to a single exponential in order to obtain an empirical binding rate K_{obs} dependent on sFcεRIα concentration. The curves serve as a model free measure for the kinetic properties in the association phase.

IgE upon FcεRI engagement (*50*) could underlie the observed biphasic kinetics.

Our study of the effects of the different IgE mutations has circumvented these uncertainties by applying model-free analysis, referring to the dependence of observed rates k_{obs} on concentration under the conditions used, fractional binding values at precise incubation times, and empirical measures indicating dissociation rates. The semiquantitative analysis performed describes general trends of the association and dissociation kinetics, under the conditions used in the experiments. This is appropriate since the dissociation and rebinding processes of IgE from the capturing antibody within the gel matrix and along the sensor surface causes small signal drifts complicating the observed kinetic process. In particular, the correction for leakage of the captured IgE and IgE−sFcεRIα is not precise enough for a detailed kinetic analysis to discriminate between possible binding mechanisms underlying the biphasic kinetics. Since our analysis does not describe the detailed process of the binding of IgE to its receptors, the obtained estimates cannot be interpreted as bimolecular rate constants. However, they allow a comparison of the effects of mutations and demonstrate that, despite the lack of a detailed molecular model for the interaction, SPR can be used in an empirical and semiquantitative way to identify the effect of mutations on the kinetics of IgE/FcεRI binding.

Mutation of Glycosylation Sites. SPR studies show that N371 is not essential for correct folding and processing of the IgE molecule in the mammalian cells since this variant showed essentially the same binding constants for FcεRI interaction as wild type and the mutation had no effect on IgE-mediated, antigen-induced cell degranulation. Like enzymatically deglycosylated IgE (*16*), it increased binding to FcεRII/CD23 more than 10-fold (Sayers et al., manuscript in preparation). In contrast, N394 appears essential for the production of a functional IgE antibody in mammalian cells since mutation of the glycosylation site at N394 inhibited binding of mutant IgE to FcεRI, as evidenced by SPR and degranulation assays. Although substitution of N by T might support O-glycosylation, our observations confirm the role

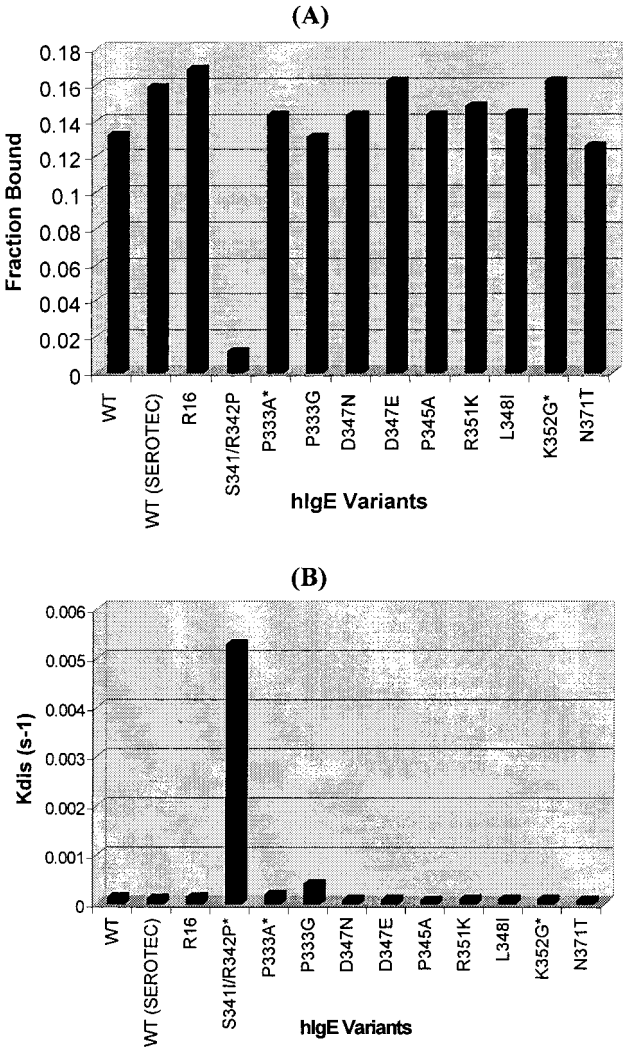

FIGURE 4: Fractional occupation of IgE sites (A) and empirical dissociation rates (B) for hIgE variants. Panel A: The fractional occupation of IgE binding sites after an injection of 600 nM sFcεRIα for 180 s was measured; the signal increase due to bound sFcεRIα was measured immediately after the injection to eliminate contributions from nonspecific binding and the refractive index contribution of the sample. This value was divided by the signal increase during the capture of IgE, and the ratio is a measure of the fractional occupation of sites. This value can be considered as a gross empirical measure of the affinity of the IgE−FcεRIα interaction since the signal of the 600 nM injection after 180 s is close to steady-state plateau binding. Panel B: The empirical dissociation rate k_d* was determined by analyzing the first 300 s of the dissociation kinetics using a single-exponential model $R(t_0)\exp[K_d^*(t - t_0)]$. These data allowed an empirical comparison of the affinity and the dissociation phase for the hIgE variant−FcεRIα interactions.

attributed to N-glycosylation by others, who demonstrated that N371Q and N265Q mutations retained FcεRI binding activity, unlike the N394Q variant (*51*). Similarly, an IgE−Fc fragment containing N265Q and N371Q mutations was shown to have binding affinities for FcεRI identical to those of native IgE (*42*). Collectively, these observations show that N394 but not T394 supports the correct folding of IgE in mammalian cells, since Fcε fragments expressed in *E. coli* recognize FcεRI and have a >10-fold increased affinity for FcεRII/CD23 (*14*−*16*).

Mutations of Residues in the A−*B Loop of Cε3.* The assignation of residues in the A−B loop in Cε3 of hIgE as a major structural determinant in IgE receptor interaction was based on previous observations, which showed that the peptide sequence Pro343−Ser353 is an essential structural determinant common to all hIgE−Fc-derived fragments that engage FcεRI (*14*). Replacement of residues conserved between rodents and man, including P345A, D347N or E, and L348I, show little influence on binding. This renders it unlikely that these residues make a direct contribution to IgE−FcεRI interaction. Nevertheless, it shows that IgE variants with substitutions at position 347 can be expressed and do not destabilize the structure of Cε3, as proposed by others (*25*). However, these substitutions do not confirm our original hypothesis that interactions between side chains of D347 and K352 make an essential contribution to FcεRI binding, since either can be replaced without any significant effect on IgE−FcεRI binding.

Collectively, these findings indicate that the overall conformation of this region, computed to form a loop constrained by invariant P residues proximal to the Cε4 domain, is critical for the correct docking of the ligand into the receptor. While N- and C-terminal truncations of the loop by only one residue effect loss of FcεRI recognition, no individual residue appears essential for binding. Others demonstrated that replacement of the A−B loop by the homologous sequence from IgG_2, which involves the insertion of an extra residue, reduces IgE−FcεRI interaction to background levels (3% positive cells) (*26*), indicating that mutations that alter the loop size inhibit receptor recognition. Further support for this notion comes from our previous observation that a disulfide bond constrained A−B loop peptide, but not a random peptide encompassing this sequence, blocks the binding of hIgE to FcεRI with an IC_{50} in the micromolar range (*15*). Similarly, chemokine−receptor interaction also depends on the recognition of a loop region in the ligand (*52*). Although cleavage at F349 by pepsin (*29*) destroys receptor recognition, our own data demonstrate that replacement of this residue by the rodent homologue Y in the context of the IgER16 chimera has virtually no effect on FcεRI interaction.

In addition to the IgE loop as the principal structural determinant in IgE−receptor interaction, an important role for additional residues in the Cε3-terminal domain is apparent, since C-terminal deletion of residues up to Pro354 is associated with a >3000-fold increase in the dissociation of truncated Fcε from cells expressing the receptor as shown in Table 2. Interestingly, additional mutations A338V, L425P, and T434A, which were introduced into the IgE S341I/R342P* variant, cause a $\sim 10^4$ decrease in binding. Since the substitution of S341I/R342P in the IgER16 variant does not inhibit FcεRI binding, replacements at these additional sites must account for the deleterious effect on receptor recognition. It would be inappropriate to suggest a direct involvement of these residues in receptor interaction, since substitution of L425 by P could introduce major structural perturbations. C-terminal truncation also reduces receptor occupancy at pH 6.4, and the pH binding profile of hIgE points to the involvement of histidine residue(s) in the C-terminal Cε3 domain in the maintenance of high affinity, making them targets for future mutagenesis studies (*14*). Involvement of Cε4-specific residues in receptor recognition can be ruled out since replacement of the Cε4 domain by the homologous Cγ3 domain is without effect on receptor recognition (*14*, *15*, *17*, *19*).

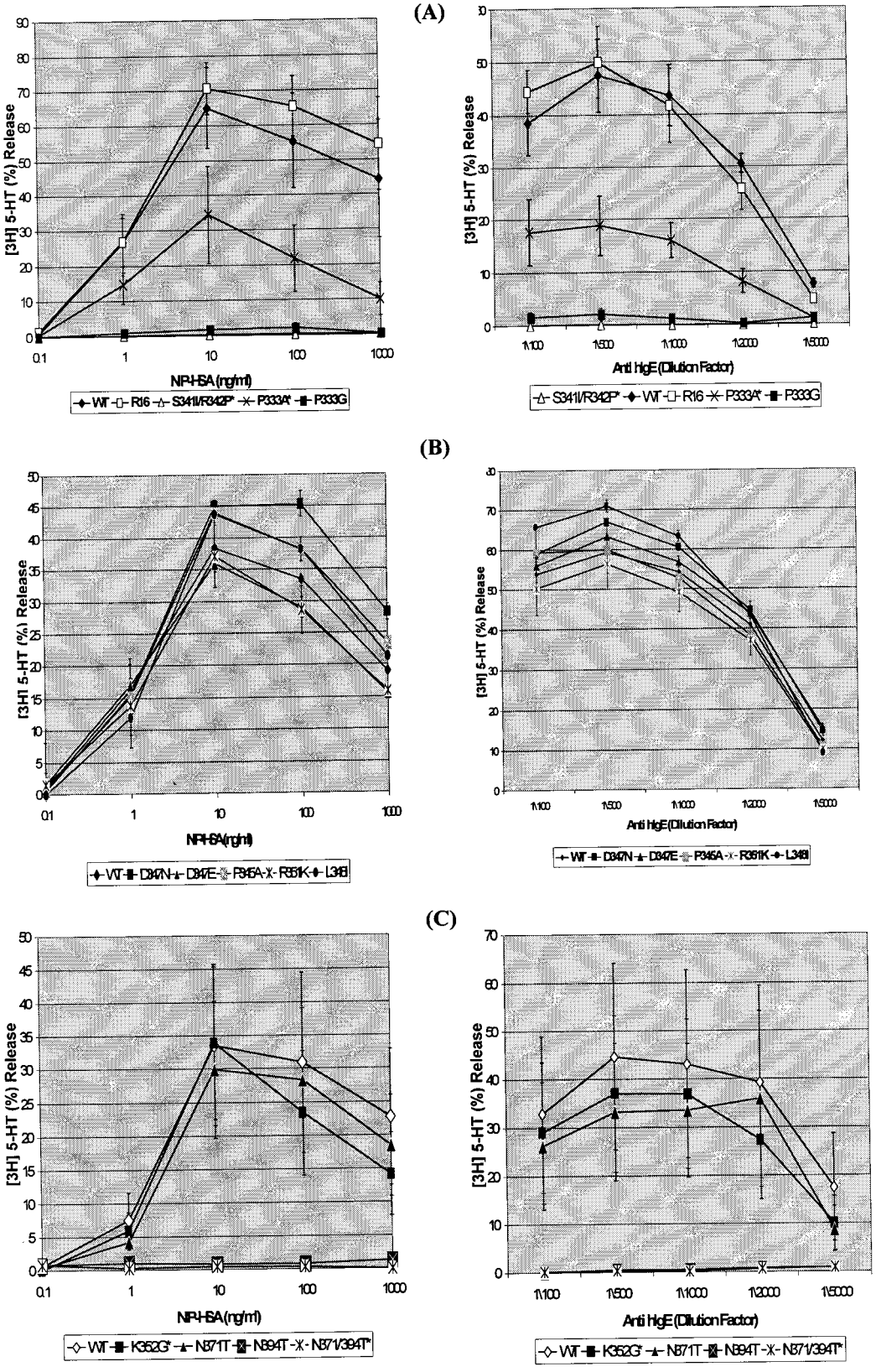

FIGURE 5: IgE variant-mediated secretion from the RBL-J41 cell line using NIP−HSA or anti-human IgE antibody challenge. The assay was performed as described in Materials and Methods. Native IgE and IgE variants were evaluated at 1 μg/mL for their ability to induce stimulus secretion coupling via the FcϵRIα chain following a dose/response challenge with increasing concentrations of NIP−HSA or anti-human IgE antisera (Dako). The data represents two independent experiments carried out in duplicate ± SEM; the percentage [3H] 5-HT secretion was calculated as previously described (*28*); and the data set was normalized to the peak endogenous secretion level (rat FcϵRIα sensitized with DNP-specific mouse IgE). The species specificity of the IgE variants was confirmed using the parental RBL-2H3.1 cell line, which expresses the rat FcϵRI complex (data not shown). All variants were unable to elicit hIgE-mediated secretion from the parental cell line.

Mutations of P333 in the Hinge Link Region between Cϵ2−3. A role for the Cϵ2−3 interface (residues 330−335) in the IgE−FcϵRI interaction has been suggested by several groups (reviewed in ref *15*). By homology with IgG, we suggested that the receptor-binding site in IgE might be found in this region. Biological activity attributed to this sequence was initially based on inhibition of PCA by IgE-derived peptides, which can give questionable interpretations (*15*). Our recent studies, which show that N-terminal Cϵ3 sequences can be deleted to L340 with only a 30-fold increase in the rate of dissociation of the ligand from the receptor (Table 2), rule out a major contribution of these residues in FcϵRI interaction. This value is in close agreement with original data published by others on the effect of mutations on residues in this interdomain segment (*53*). In their recent reevaluation of these data, they suggested that mutation of R334S effects a 120-fold increase in ligand dissociation (*25*). The reason for the choice of substitution of R by S is not apparent, since replacement by K and E might be more appropriate. Their suggestion that R334 forms part of a significant contact with the receptor (*25*) is questionable since the inter-Cϵ2−3 linker region can be deleted, while the truncated ligand still binds FcϵRI with high affinity (*14*).

We focused on the role of P333 since FRET measurements suggested that rat IgE bends out of plane in this region (*54*). Structures with proline tend to be more inflexible since there are fewer possible conformational states. If IgE interacts with the receptor in a bent conformation, P in the hinge might be critical. To determine whether this residue contributes to the interaction by a restriction on structure, P333 was replaced by A and G. As shown in Figure 4B, SPR kinetic analysis showed only a modest increase in the dissociation rate for both mutants as compared to the native IgE molecule, and both ligands recognize cellular hFcϵRI with high affinity (Table 2).

In contrast, a striking decrease in the ability of the P333-mutated IgE molecules to support aggregation of FcϵRI was observed. P333A reduced mediator release by 50%, while P333G could not mediate degranulation. (Figure 5A). A comparison of NIP−HSA and anti-hIgE-mediated aggregation demonstrated (Figure 5A) that this failure is not influenced by the nature of the cross-linking stimulus. These observations are unexpected in view of the small effects of the P333 mutations on the kinetics of IgE−FcϵRI interaction and are difficult to reconcile with the notion that, once receptor sensitization occurs, secretory responses can be initiated by clustering adjacent receptors via cognate antigen or anti-IgE (*55*, *56*). They disagree with earlier suggestions that the persistence of FcϵRI-mediated signal transduction is directly related to the intrinsic affinity of the ligand for the receptor (*57*). It has, however, been suggested that orientational constraints can affect the mobility and state of aggregation of the receptor and that this determines secretory responses. Of particular interest in this respect is the work by Pecht and collaborators (*49*, *58*−*61*), who compared IgE-mediated stimulus secretion coupling in response to monoclonal antibodies. Their work suggests that the capacity to induce mediator release is not a function of the affinity of the cross-linker for the ligand but depends on the assembly of aggregated receptors into immobile species (*59*). Their observation, that the rigidity of IgE/anti-IgE correlates with the capacity to trigger mast cell exocytosis, is directly relevant to our findings, which demonstrate that a progressive decrease in the capacity of hIgE variants to mediate mast cell degranulation parallels the relief of structural constraints computed to occur as a result of exchange of P by A and G. It is interesting to note that others conclude that P333 plays no role in IgE−FcϵRI interaction (*23*), since its mutation is associated with a <7-fold increase in dissociation. Unfortunately, no information was published relating to the ability of this variant to mediate degranulation. In contrast, P345A mutation does not alter effector functions of IgE, highlighting the critical role of P333A/G mutations in the ligand's ability to couple a cross-linking stimulus to mediator secretion. The effects we observe point to a progressive loss of entropic constraints, which have been computed to introduce a bend into the structure of the interdomain region between Cϵ2−3 (*21*).

A more detailed understanding of the molecular basis of this surprising observation may yield useful information for the design of FcϵRI blocking agents, which cannot induce mediator secretion upon cross-linking with allergen or anti-IgE and provide new insights into the nature of receptor-mediated transmembrane signaling events. This could be of general and specific pharmacological importance.

ACKNOWLEDGMENT

We appreciated helpful discussion with Drs. E. M. Carey (MBB, University of Sheffield) and A. C. Spivey (Department Chemistry, University of Sheffield). This work has benefited from the availability of the BBSRC protein sequencing facility in Aberdeen, U.K.

REFERENCES

1. Capron, A., Dessaint, J. P., Capron, M., Joseph, M., Ameisen, J. C., and Tonnel, A. B. (1986) *Immunology Today 7*, 15−18.
2. Hagan, P., Blumenthal, U. J., Dunn, D., Simpson, A. J. G., and Wilkins, H. A. (1991) *Nature 349*, 243−245.
3. Holgate, S. T. (1997) *Lancet 350* (Suppl. II), 5−9.
4. Stanworth, D. R., Humphrey, J. H., and Bennich, H. H. (1968) *Lancet 2*, 17−18.
5. Stanworth, D. R., Jones, V. M., Lewin, I. V., and Nayyar, S. (1990) *Lancet 336*, 12791281.
6. Ishizaka, K., Ishizaka, T., and Lee-E. H. (1970) *Immunochemistry 7*, 687−702.
7. Kenten, J., Helm, B., Ishizaka, T., Cattini, P., and Gould, H. (1984) *Proc. Natl. Acad. Sci. U.S.A. 81*, 2955−2950.
8. Lui, F. T., Albrandt, K. A., Bry, C. G., and Ishizaka, T. (1984) *Proc. Natl. Acad. Sci. U.S.A. 81*, 5369−5373.
9. Geha, R. S., Helm, B., and Gould, H. (1985) *Nature 315*, 577−578.
10. Coleman, J. W., Helm, B. A., Stanworth, D. R., and Gould, H. J. (1985) *Eur. J Immunol. 15*, 966−969.
11. Ishizaka, T., Helm, B., Hakimi, J., Niebyl, J., Ishizaka, K., and Gould, H. (1986) *Proc. Natl. Acad. Sci. U.S.A. 83*, 8323−8327.
12. Helm, B., Marsh, P., Vercelli, D., Padlan, E., Gould, H., and Geha, R (1988) *Nature 331*, 181−183.
13. Helm, B. A., Kebo, D., Vercelli, D., Glovsky, M. M., Gould, H. J., Ishizaka, K., Geha, R., and Ishizaka, T. (1989) *Proc. Natl. Acad. Sci. U.S.A. 186*, 9465−9469.
14. Helm, B. A., Sayers, I., Higginbottom, A., Machado, D. C., Ling, Y., Ahmad, K., Padlan, E. A., and Wilson, A. P. M (1996) *J. Biol. Chem. 271*, 7494−7500.
15. Helm B. A., Spivey, A. C., and Padlan, E. A. (1997) *Allergy 52*, 1155−1169.
16. Vercelli, D., Helm, B., Marsh, P., Padlan, E., Geha, R. S., and Gould, H (1989) *Nature 338*, 649−651.

17. Weetall, M., Shopes, B., Holowka, D., and Baird, B. (1990) *J. Immunol. 145*, 3849−3854.
18. Nissim, A., and Eshhar, Z. (1991) *Int. Arch. Allergy Appl. Immunol. 94*, 93−95.
19. Nissim, A., Eshhar, Z. (1992) *Mol. Immunol. 29*, 1065−1072.
20. Nissim, A., Schwarzbaum, S., Siraganian, R., and Eshhar, Z. (1993) *J. Immunol. 150*, 1365−1374.
21. Helm, B. A., Ling, Y., Teale, C., Padlan, E. A., and Bruggemann, M. (1991) *Eur. J. Immunol. 21*, 1543−1548.
22. Duncan, A. R., Woof, J. M., Partridge, L. J., Burton, D. R., and Winter, G. (1988) *Nature 332*, 563−564.
23. Beavil, A. J., Beavil, R. L., Chan, C. M. W., Cook, J. P. D., Gould, H. J., Henry, A. J., Owens, R. J., Shi, J., Sutton, B. J., and Young, R. J. (1993) *Biochem. Soc. Trans. 21*, 968−972.
24. Sutton, B. J., and Gould, H. J. (1993) *Nature 366*, 421−428.
25. Henry, A. J., Cook, P. D., McDonnell, J. M., Mackay, G. A., Shi, J., Sutton, B. J., and Gould, H. J. (1997) *Biochemistry 36*, 15568−15578.
26. Presta, L., Shields, R., O'Connell, L., Lahr, S., Porter, J., Gorman, C., and Jardieu, P. (1994) *J. Biol. Chem. 269*, 26368−26373.
27. Marsh, P., Helm, B. A., and Gould, H. J. (1989) *IgE in allergic inflammation* (Johansson, S. G. O., Ed.) pp 26−31, Pharmacia Allergy Research Foundation, Uppsala, Sweden.
28. Wilson, A. P., Pullar, C., Camp, A., and Helm, B. A. (1993) *Eur. J Immunol. 23*, 240−244.
29. Lindstrom-Bahr, H. (1974) Ph.D. Thesis, University of Uppsala.
30. Neuberger, M. S., Williams, G. T., Mitchell, E. B., Jouhal, S. S., Flanagan, J. G., and Rabbitts, T. H. (1985) *Nature 314*, 268−270.
31. Brueggemann, M., Williams, G., Bindon, C., Clark, M., Walker, M., Jefferis, R., Waldmann, H., and Neuberger, M. (1987) *J. Exp. Med. 166*, 1351−1361.
32. Padlan, E. A., and Davies, D. R. (1986) *Mol. Immunol. 23*, 1063−1075.
33. Deisenhofer, J. (1981) *Biochemistry 20*, 2361−2370.
34. Kulczycki, A., Isersky, C., and Metzger, H. (1974) *J. Exp. Med. 139*, 600−616.
35. Kabat, E. A., Wu, T. T., Reid-Miller, M., Perry, H. M., and Gottesmann, K. S. (1991) *Sequences of Proteins of Immunological Interest*, 5th ed., U.S. Department of Health and Human Services, Washington, DC.
36. Helm, B. A., Sayers, I.; Swan, J., Smyth, L. J. C., Cain, S. A., Suter, M., Machado, D. C., Spivey, A. C., and Padlan, E. A. (1998) *Technol. Health Care*, in press.
37. Bingham, B. R., Monk, P. N., and Helm, B. A. (1994) *J. Biol. Chem. 269*, 19300−19306.
38. Karlsson, R., Michaelsson, A., and Mattsson, L. (1991) *J. Immunol. Methods 145*, 229−240.
39. Miller, L., Blank, U., Metzger, H., and Kinet, J. P. (1989) *Science 244*, 434−437.
40. Hakimi, J., Seals, C., Kondas, J. A., Pettine, L., Danho, W., & Kochan, J. (1991) *J. Biol. Chem. 265*, 22079−22081.
41. Basu, M., Hakimi, J., Dharm, E., Kondas, J. A., Tsien, W. H., Pilson, R. S., Lin, P., Gilfillan, A., Haring, P., Braswell, E. H., Nettleton, M. Y., and Kochan, J. P. (1993) *J. Biol. Chem. 268*, 13118−13127.
42. Young, R. J., Owens, R. J., Mackay, G..A., Chan, C..M. W., Shi, J., Hide, M., Francis, D. M., Henry, A. J., Sutton, B. J., and Gould, H. J. (1995) *Protein Eng. 8*, 193−199.
43. Schuck, P., and Minton, A. P. (1996) *Trends Biochem. Sci. 252*, 458−460.
44. Schuck, P. (1997) *Annu. Rev. Biophys. Biomol. Struct. 26*, 541−566.
45. Schuck, P., and Minton, A. P. (1996) *Anal. Biochem. 240*, 262−272.
46. O'Shannessy, D. J., and Winzor, D. J. (1996) *Anal. Biochem. 236*, 275−283.
47. Minton, A. P. (1980) *Mol. Pharmacol. 19*, 1−14.
48. Schuck, P., Milar, D. B., and Kort, A. A. (1998) *Anal. Biochem.*, in press.
49. Ortega, E., Schweitzer-Stenner, R., and Pecht, I. (1991) *Biochemistry 30*, 3473−3483.
50. Sechi, S., Roller, P. P., Willette-Brown, J., and Kinet, J. P. (1996) *J. Biol. Chem. 271*, 19256−19263.
51. Nettleton, M. Y., and Kochan, J. P. (1995) *Int. Arch. Allergy Immunol. 107*, 328−329.
52. Clark-Lewis, I., Kim, K. S., Rajarathnam, K., Gong, J. H., Dewald, B., Moser, B., Baggiolini, M., and Sykes, B. D. (1995) *J. Leukocyte Biol. 57*, 703−711.
53. McDonnell, J. M., Beavil, A. J., Mackay, G. A., Henry, A. J., Cook, J. P. D., Gould, H. J., and Sutton, B. J. (1997) *Biochem. Soc. Trans. 25*, 387−392.
54. Zheng, Y., Shopes, B., Holowka, D., and Baird, B (1991) *Biochemistry 30*, 9125−9132.
55. Ishizaka. T., and Ishizaka, K. (1984) *Prog. Allergy 34*, 188−235.
56. Metzger, H., Alcaraz, G., Hohman, R., Kinet, J. P., Pribluda, V., and Quarto, R. (1986) *Annu. Rev. Immunol. 4*, 419−470.
57. Kent, U. M. Mao, S. Y., Wofsy., C., Goldstein, B., Ross, S., and Metzger, H. (1994) *Proc. Natl. Acad. Sci. U.S.A. 91*, 3087−3091.
58. Ortega, E., Schweitzer-Stenner, R., and Pecht, I. (1988) *EMBO J. 7*, 4101−4109.
59. Pecht, I., Ortega, E., and Jouvin, T. M. (1991) *Biochemistry 30*, 3450−3458.
60. Schweitzer-Stenner, R., and Pecht, I. (1994) *Biochemistry 33*, 8813−8825.
61. Schweitzer-Stenner, R., Tamir, I., and Pecht, I. (1997) *Biophys. J. 72*, 2470−2478.

BI981456K